

Fast List Decoders for Polarization-Adjusted Convolutional (PAC) Codes

Hongfei Zhu, Zhiwei Cao, Yuping Zhao, Dou Li, Yanjun Yang, Yiru Wang and Zongren Guo

Abstract—A latest coding scheme named polarization-adjusted convolutional (PAC) codes is shown to approach the dispersion bound for the code (128,64) under list decoding. However, to achieve the near-bound performance, the list size of list decoding needs to be excessively large, which leads to insufferable latency. In this paper, to improve the speed of list decoding, fast list decoders for PAC codes are proposed. We define four types of constituent nodes and provide fast list decoding algorithms for each of them. Simulation results present that fast list decoding with three types of constituent nodes can yield exactly the same error-correction performance as list decoding, and reduce more than 50% time steps for the code (128,64). Moreover, fast list decoding with four types of constituent nodes can further reduce decoding latency with negligible performance degradation.

Index Terms—Polarization-adjusted convolutional codes, polar codes, list decoding, constituent nodes, dispersion bound.

I. INTRODUCTION

POLAR codes are the first family of error-correcting codes with provable capacity-achieving property for systematic binary-input discrete memoryless channels (BI-DMCs) [1]. The successive cancellation (SC) decoding is one of the most common decoding algorithms of polar codes with a low complexity $O(N \log_2 N)$, where N is the code length. However, there are two main drawbacks associated with SC. Firstly, polar codes decoded with SC achieve the channel capacity only when N approaches infinity. For practical polar codes of short to moderate lengths, SC falls short in providing satisfactory error-correction performance. Secondly, the serial decoding nature of SC results in low throughput and high latency, and one codeword consumes $2N-2$ time steps without resource constraints [2].

In order to reduce the performance gap between SC and maximum likelihood (ML), the SC List (SCL) decoding algorithm was introduced in [3]. Instead of focusing on a single candidate codeword like SC, the L most probable candidate codewords are allowed to survive concurrently. Under SCL decoding, it was shown that polar codes concatenated with a cyclic redundancy check (CRC) can outperform low-density parity-check (LDPC) codes of the similar length. While SCL provides better error-correction performance than SC, it comes at the cost of lower throughput and higher latency, requiring $2N-2+K$ time steps to be completed, where K is the number of information bits [4].

Various attempts have been made to improve the speed of SCL decoding. Among these methods, tree pruning was shown

to be extremely effective. Four types of constituent nodes, namely rate zero (Rate-0) node with all frozen bits, rate one (Rate-1) node with all information bits, repetition (Rep) node with a single information bit in the most reliable position, and single parity-check (SPC) node with a single frozen bit in the least reliable position, were capable of being decoded in parallel with low-complexity decoding algorithms. Based on the four special nodes, simplified SCL (SSCL) [5] and SSCL-SPC [6] increased the throughput and reduced the latency significantly with negligible error-correction performance loss with respect to SCL. Nonetheless, SSCL and SSCL-SPC failed to address the redundant path split associated with a specific list size. Therefore, Fast-SSCL [7] and Fast-SSCL-SPC [8] provided a more efficient algorithm for Rate-1 and SPC nodes, respectively. These state-of-the-art algorithms can further reduce the number of path forks and guarantee the error-correction performance preservation.

Recently in [9], a new coding scheme named polarization-adjusted convolutional (PAC) codes were proposed. They rely on the concatenation a convolutional transform [10] with the polarization transform. The message bits are first encoded using a one-to-one convolutional operation and then transmitted over polarized synthetic channels. Remarkably, under Fano sequential decoding [11], the performance of PAC codes with length 128 and rate 1/2 can reach the finite-length capacity bound a.k.a. dispersion bound [12]. Later in [13] and [14], the authors independently proposed the list decoding for PAC codes. Compared with sequential decoding, list decoding is a non-backtracking tree search approach with a fixed complexity. Moreover, it is certainly advantageous in terms of worst-case complexity and at low signal-to-noise ratios (SNRs). However, to achieve the same performance as sequential decoding, the list size of list decoding needs to be excessively large ($L \geq 256$), leading to insufferable latency.

In this paper, to alleviate the tremendous latency of list decoding, we propose fast list decoders for PAC codes. Four types of constituent nodes are defined, namely Rate-0 nodes, Rate-1 nodes, Rev (reversal) nodes and SPC nodes. For each constituent node, its fast list decoding algorithm is provided along with necessary proofs. Numerical results illustrate that fast list decoding with three types of constituent nodes, i.e., Rate-0, Rate-1 and Rev nodes provides an exact match to list decoding with no error-correction performance loss. In addition, the number of time steps can be significantly reduced. Moreover, the introduction of SPC nodes further improves the latency and results in neglectable performance degradation.

The remainder of this paper is organized as follows: Section II provides a background on PAC codes and list decoding.

The authors are with the School of Electronics Engineering and Computer Science, Peking University, Beijing 100871, China (e-mail: {zhuhongfei, cao_zhiwei, yuping.zhao, lidou, yangyj}@pku.edu.cn; 2001111274@stu.pku.edu.cn; 1901213311@pku.edu.cn).

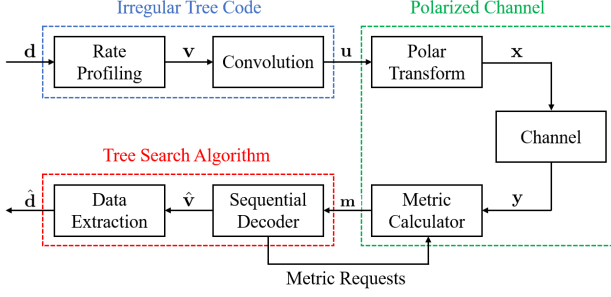


Fig. 1. PAC coding scheme.

Section III introduces the proposed fast list decoders for PAC codes. Simulation results are provided in Section IV. Finally, Section IV draws the main conclusions of the paper.

II. BACKGROUND

A. PAC Codes

The PAC coding scheme is shown in Fig. 1. A PAC code is specified by four parameters $(N, K, \mathcal{A}, \mathbf{c})$, where N is the codeword length, K is the length of information bits, \mathcal{A} is the index set of information bits, and \mathbf{c} is the impulse response of convolution. The codeword length is constrained to be a power of two, i.e., $N = 2^n$ for $n \geq 1$, just as polar codes. The code rate is denoted as $R = K/N$.

At the transmitter, a rate-profiling block inserts the source word $\mathbf{d} = (d_0, d_1, \dots, d_{K-1})$ into a data carrier word $\mathbf{v} = (v_0, v_1, \dots, v_{N-1})$ in accordance with a information bits set \mathcal{A} so that $\mathbf{v}_{\mathcal{A}} = \mathbf{d}$ and $\mathbf{v}_{\mathcal{A}^c} = \mathbf{0}$. The PAC codeword $\mathbf{x} = (x_0, x_1, \dots, x_{N-1})$ is obtained from \mathbf{v} by the one-to-one transformation $\mathbf{x} = \mathbf{vTP}_n$ where \mathbf{T} is a convolution operation and \mathbf{P}_n is the polar transform defined as the n -th Kronecker power of $\mathbf{P} = [1, 0; 1, 1]$, i.e., $\mathbf{P}_n = \mathbf{P}^{\otimes n}$ ($n = \log_2 N$). As usual, we characterize the convolution operation by an impulse response $\mathbf{c} = (c_0, c_1, \dots, c_m)$, where by convention we assume that $c_0 = 1$ and $c_m = 1$. The number of states of the convolutional shift register is 2^m and the parameter $m+1$ is called the constraint length of the convolution.

The vector \mathbf{x} is transmitted through a noisy channel and received as the vector \mathbf{y} . At the receiver, Fano sequential decoding [11] of the underlying convolutional code can be employed to decode the data carrier vector \mathbf{v} . Notably, the path metrics at the input to the sequential decoder are obtained via repeated calls to the SC decoder for the underlying polar code. The performance of PAC codes is more sensitive to the choice of \mathcal{A} than to \mathbf{c} , and the RM rule [15], [16] was shown to be the best method to design \mathcal{A} in terms of frame error rate (FER) performance [9].

B. List Decoding of PAC Codes

Sequential decoding is a backtracking search algorithm with unfixed complexity varying with SNRs. Representing PAC codes as the special case of polar codes with dynamically frozen bits [17], the authors in [13] and [14] independently put forward a non-backtracking search algorithm with fixed

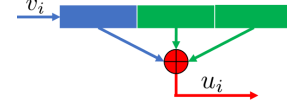
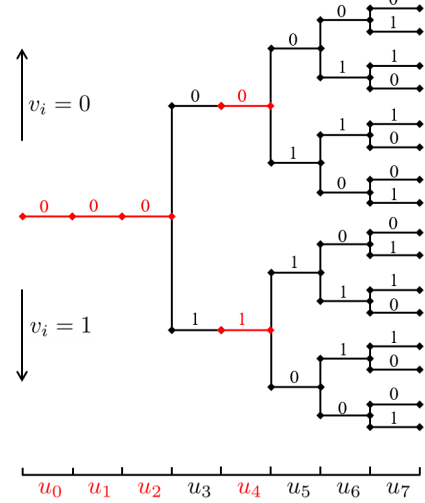
Fig. 2. The shift register corresponding to $\mathbf{c} = (1, 1, 1)$.

Fig. 3. Irregular code tree of the rate-1 convolutional code inside the PAC code.

complexity named list decoding for PAC codes. Since PAC codes combine convolution and polar mapping, the list decoding process of PAC codes consists of two trees: code tree for convolutional codes and binary tree for polar codes. In the following, we take $\text{PAC}(8, 4, \{3, 5, 6, 7\}, (1, 1, 1))$ for example.

1) *Code Tree for Convolutional Codes*: Fig. 2 displays the shift register corresponding to $\mathbf{c} = (1, 1, 1)$. Note that the state of the register resets before each codeword enters. Under the frozen-bit constraint imposed by rate-profiling, the rate-1 convolutional code yields an irregular code tree, which is illustrated in Fig. 3. The code tree branches only when there is a new information bit $v_i, i \in \mathcal{A}$ going into the register. When there is branching in the code tree at some stage $i \in \mathcal{A}$, by convention, the upper branch corresponds to $v_i = 0$ and the lower branch corresponds to $v_i = 1$. Other nodes of the code tree are in one-to-one correspondence with the convolution input words \mathbf{v} satisfying the constraint $\mathbf{v}_{\mathcal{A}^c} = \mathbf{0}$.

2) *Binary Tree for Polar Codes*: The binary tree of the polar code inside the PAC code is presented in Fig. 4. Given a node o of width $N_o = 2^{n-d_o}$ at depth d_o in the binary tree, we use \mathcal{V}_o to denote the set of nodes of the subtree rooted at node o . We let $I(o)$ denote the index of a leaf node o . Furthermore, to each node o we associate the set

$$\mathcal{I}_o = \{I(q) : q \in \mathcal{V}_o \text{ and } q \text{ is a leaf node}\} \quad (1)$$

containing the indices of all leaf nodes that are descendants of node o . Unless specified, we use $\boldsymbol{\alpha} = \{\alpha_0, \dots, \alpha_{N_o-1}\}$, $\boldsymbol{\beta} = \{\beta_0, \dots, \beta_{N_o-1}\}$, $\mathbf{u} = \{u_0, \dots, u_{N_o-1}\}$, and $\mathbf{v} = \{v_0, \dots, v_{N_o-1}\}$ to denote the LLR vector on the top of the subtree, the bit vector on the top of the subtree, the bit

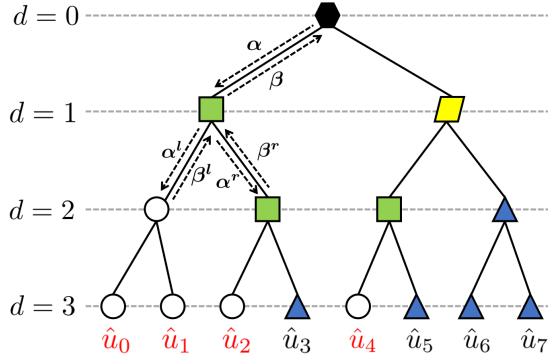


Fig. 4. Binary tree of the polar code inside the PAC code. White circles are Rate-0 nodes, blue triangles are Rate-1 nodes, green squares are Rev nodes, yellow parallelograms are SPC nodes and black hexagons are general nodes.

vector at the bottom of the subtree, and the message vector corresponding to \mathbf{u} , respectively. Additionally, \mathbf{P}_{n-d_o} is the $(n - d_o)$ -th Kronecker power of $\mathbf{P} = [1, 0; 1, 1]$ and \mathbf{s} is the state vector of the shift register consisting of m bits. Note that the inverse of \mathbf{P}_{n-d_o} is itself [18].

The SC decoding process for the polar code can be depicted as follows. The vertex node at depth $d = 0$ of the decoding tree is fed with the log-likelihood ratio (LLR) values received from the channel. Subsequently for each node o , the soft LLR values in α are passed from a parent node to its child nodes and the hard bits in β are passed from the opposite direction. The elements of the left messages $\alpha^l = \{\alpha_0^l, \dots, \alpha_{\frac{N_o}{2}-1}^l\}$ and right messages $\alpha^r = \{\alpha_0^r, \dots, \alpha_{\frac{N_o}{2}-1}^r\}$ are calculated as

$$\alpha_i^l = \text{sgn}(\alpha_i) \cdot \text{sgn}(\alpha_{i+\frac{N_o}{2}}) \cdot \min(|\alpha_i|, |\alpha_{i+\frac{N_o}{2}}|) \quad (2)$$

$$\alpha_i^r = (1 - 2\beta_i^l) \cdot \alpha_i + \alpha_{i+\frac{N_o}{2}}; \quad (3)$$

while the elements of β are computed using the left messages $\beta^l = \{\beta_0^l, \dots, \beta_{\frac{N_o}{2}-1}^l\}$ and right messages $\beta^r = \{\beta_0^r, \dots, \beta_{\frac{N_o}{2}-1}^r\}$

$$\beta_i = \begin{cases} \beta_i^l \oplus \beta_i^r, & \text{if } i < \frac{N_o}{2} \\ \beta_{i-\frac{N_o}{2}}^r, & \text{otherwise} \end{cases} \quad (4)$$

3) *Path Split*: At the beginning of list decoding, there is a single path in the list. A path metric (PM) is associated to each path and the process of path split is described as follows:

- When the index of the current bit v_i is in the set \mathcal{A}^c , the decoder knows its value, usually $v_i = 0$ and therefore it is encoded into u_i based on the impulse response \mathbf{c} and the current state \mathbf{s} of the shift register. Then the PM of the i -th bit for the l -th path is computed as

$$\text{PM}_{i_l} = \begin{cases} \text{PM}_{i-l}, & \text{if } \hat{u}_{i_l} = \frac{1}{2}(1 - \text{sgn}(\alpha_{i_l})) \\ \text{PM}_{i-l} + |\alpha_{i_l}|, & \text{otherwise} \end{cases} \quad (5)$$

Whereafter the shift register of the l -th path is updated and u_i is fed back into the SC decoder as mentioned in Section II-B2.

- If the index of the current bit v_i is in the set \mathcal{A} , there are two options for v_i , i.e., $v_i = 0$ and 1. For each option of

Algorithm 1 Fast List Decoding of a Rate-0 Node o

Input: $\alpha[l], \mathbf{s}[l], \text{PM}_l, l = 0, \dots, L-1, \mathbf{P}_{n-d_o}, \mathbf{c}$

Output: $\beta[l], \mathbf{s}[l], \text{PM}_l, \hat{\mathbf{v}}[l], \hat{\mathbf{u}}[l], l = 0, \dots, L-1$

```

1: for  $l \leftarrow 0$  to  $L-1$  do
2:   for  $i \leftarrow 0$  to  $N_o-1$  do
3:      $\hat{v}_i[l] \leftarrow 0$ 
4:      $[\hat{u}_i[l], \mathbf{s}[l]] \leftarrow \text{conv1bitEnc}(\hat{v}_i[l], \mathbf{s}[l], \mathbf{c})$ 
5:   end for
6:    $\beta[l] \leftarrow \hat{\mathbf{u}}[l] \cdot \mathbf{P}_{n-d_o}$ 
7:    $\text{PM}_l \leftarrow \text{calcPM}(\text{PM}_l, \alpha[l], \beta[l], N_o)$ 
8: end for

```

0 and 1, the aforementioned process for $i \in \mathcal{A}^c$ including convolutional transform, state update and SC process. We can see that at every estimation for information bits, the number of paths doubles. Hence, in order to limit the increase in the complexity, only the L paths with lowest PMs survive while others are discarded.

Simulation results demonstrate that list decoding has distinct advantages over sequential decoding in certain scenarios such as low-SNR regimes or situations where the worst-case complexity/latency is the primary constraint [14]. Furthermore, PAC codes using list decoding can also approach dispersion bound of length 128 and rate 1/2, just as sequential decoding [13], [14]. However, the near-bound performance of list decoding requires extremely large list size ($L \geq 256$), leading to considerable latency which is not feasible in practice. Therefore, based on Fast-SSCL-SPC algorithm for polar codes [8], we propose fast list decoders for PAC codes as presented in the following.

III. FAST LIST DECODERS FOR PAC CODES

It is known that for polar codes, PMs rely on the LLR values at the top of the binary tree identified by their constituent nodes: thus, it is not necessary to traverse the tree to compute them [6]. In this section, we define four types of constituent nodes for PAC codes, namely Rate-0 nodes, Rate-1 nodes, Rev nodes and SPC nodes. For each constituent node, its fast list decoding algorithm is provided along with necessary proofs. Subroutines inside all algorithms are provided in Appendix A. Eventually, compared with list decoding, time steps of fast list decoding for each constituent node are analyzed.

A. Rate-0 Nodes

We say that a node o is a Rate-0 node with respect to \mathcal{A}^c if $\mathcal{I}_o \in \mathcal{A}^c$, i.e., if all bits in \mathbf{v} are frozen bits. For each path, when SC decoding reaches a rate-0 node o plotted in white circles in Fig. 4, it can immediately set $\mathbf{v} = \mathbf{0}$ without utilizing α to activate its children. Then \mathbf{u} can be obtained through convolutional encoding and β can be computed using polar encoding. Finally, PMs are updated using α and β following the same formula as (5). Notice that no path split is needed for Rate-0 nodes. Algorithm 1 illustrates the concrete steps.

Algorithm 2 Fast List Decoding of a Rate-1 Node o

Input: $\alpha[l], s[l], PM_l, l = 0, \dots, L-1, \mathbf{P}_{n-d_o}, \mathbf{c}$
Output: $\beta[l], s[l], PM_l, \hat{\mathbf{v}}[l], \hat{\mathbf{u}}[l], l = 0, \dots, L-1$

```

1: for  $l \leftarrow 0$  to  $L-1$  do
2:    $\beta[l] \leftarrow \frac{1}{2}(1 - \text{sgn}(\alpha[l]))$ 
3:    $[|\tilde{\alpha}[l]|, \tilde{\mathbf{I}}[l]] \leftarrow \text{sort}(|\alpha[l]|, \text{'ascend'})$ 
4: end for
5: for  $i \leftarrow 0$  to  $\min(L-1, N_o) - 1$  do
6:   for  $l \leftarrow 0$  to  $L-1$  do
7:      $ll = l + L$ 
8:      $[\beta'[l], \beta'[ll]] \leftarrow [\beta[l], \beta[l]]$ 
9:      $[s'[l], s'[ll]] \leftarrow [s[l], s[l]]$ 
10:     $[\tilde{\alpha}'[l], \tilde{\alpha}'[ll]] \leftarrow [\tilde{\alpha}[l], \tilde{\alpha}[l]]$ 
11:     $[\tilde{\mathbf{I}}'[l], \tilde{\mathbf{I}}'[ll]] \leftarrow [\tilde{\mathbf{I}}[l], \tilde{\mathbf{I}}[l]]$ 
12:     $[\tilde{\beta}'_i[l], \tilde{\beta}'_i[ll]] \leftarrow [0, 1]$ 
13:     $PM'_l \leftarrow \text{calcPM}(PM_l, \tilde{\alpha}'_i[l], \tilde{\beta}'_i[l], 1)$ 
14:     $PM'_{ll} \leftarrow \text{calcPM}(PM_l, \tilde{\alpha}'_i[ll], \tilde{\beta}'_i[ll], 1)$ 
15:   end for
16:    $[\widetilde{\mathbf{PM}}, \tilde{\mathbf{l}}] \leftarrow \text{sort}([PM'_0, \dots, PM'_{2L-1}], \text{'ascend'})$ 
17:   for  $l \leftarrow 0$  to  $L-1$  do
18:      $PM_l \leftarrow \widetilde{PM}_l$ 
19:      $\tilde{\mathbf{I}}[l] \leftarrow \tilde{\mathbf{I}}'[l]$ 
20:      $\tilde{\alpha}[l] \leftarrow \tilde{\alpha}'[l]$ 
21:      $s[l] \leftarrow s'[l]$ 
22:      $\beta[l] \leftarrow \beta'[l]$ 
23:      $\beta_{\tilde{\mathbf{I}}[l]}[l] \leftarrow \beta'_{\tilde{\mathbf{I}}[l]}[l]$ 
24:   end for
25: end for
26: for  $l \leftarrow 0$  to  $L-1$  do
27:    $\hat{\mathbf{u}}[l] \leftarrow \beta[l] \cdot \mathbf{P}_{n-d_o}$ 
28:   for  $i \leftarrow 0$  to  $N_o - 1$  do
29:      $[\hat{v}_i[l], s[l]] \leftarrow \text{conv1bitInvEnc}(\hat{u}_i[l], s[l], \mathbf{c})$ 
30:   end for
31: end for
```

B. Rate-1 Nodes

We say that a node o is a Rate-1 node with respect to \mathcal{A} if $\mathcal{I}_o \in \mathcal{A}$, i.e., if all bits in \mathbf{v} are information bits. In Fig. 4, Rate-1 nodes are plotted in blue triangles. The process of path split can be carried out on the top of the subtree following the same rule as illustrated in Section II-B3. Although a Rate-1 node o with width N_o contains N_o information bits, the minimum number of path splits incurring no error-correction performance loss is $\min(L-1, N_o)$, where L is the list size of list decoding [7]. Other bits in β can be directly judged by their corresponding LLRs in α . After β is obtained, \mathbf{u} can be calculated through the inverse process of polar encoding and subsequently \mathbf{v} can be calculated through the inverse process of convolutional encoding. We give the pseudo-code in Algorithm 2.

C. Rev Nodes

We say that a node o is a Rev node if the first $N_o - 1$ bits in \mathbf{v} are frozen bits while the last bit v_{N_o-1} is an information bit. The Rev nodes are depicted in green squares in Fig. 4.

Lemma 1: The elements of the last row of $\mathbf{P}_n, n \geq 1$ are all ones.

Proof: We prove this lemma by induction. When $n = 1$, we have $\mathbf{P}_1 = \mathbf{P} = [1, 0; 1, 1]$, the lemma holds. Supposing that this lemma holds for $n-1, n \geq 2$, then we have

$$\begin{aligned}
 \mathbf{P}_n &= \mathbf{P} \otimes \mathbf{P}_{n-1} \\
 &= \begin{pmatrix} 1 & 0 \\ 1 & 1 \end{pmatrix} \otimes \mathbf{P}_{n-1} \\
 &= \begin{pmatrix} \mathbf{P}_{n-1} & \mathbf{0} \\ \mathbf{P}_{n-1} & \mathbf{P}_{n-1} \end{pmatrix}
 \end{aligned} \tag{6}$$

It can be seen that the last row of \mathbf{P}_n is constructed by concatenation the last row of \mathbf{P}_{n-1} twice. Since we have assumed that the elements of the last row of \mathbf{P}_{n-1} are all ones, the elements of last row of \mathbf{P}_n are also all ones. ■

Based on Lemma 1, we can obtain the following theorem for Rev nodes.

Theorem 1: As for a Rev node o , Assuming that β_0 is the bit vector corresponding to $v_{N_o-1} = 0$ while β_1 corresponds to $v_{N_o-1} = 1$, then we have

$$\beta_0 \oplus \beta_1 = \mathbf{0} \tag{7}$$

Proof: We have known that the first $N_o - 1$ bits in \mathbf{v} are fixed to zeros, i.e., $v_i = 0, i = 0, \dots, N_o - 2$ while only the last bit have two values, i.e., $v_{N_o-1} = 0$ or 1. Moreover, in Section II-A we have assumed that the first element in \mathbf{c} is 1, i.e., $c_0 = 1$. Therefore, after N_o -bit convolutional encoding, two cases of \mathbf{u} will only differ in the last bit u_{N_o-1} while the first $N_o - 1$ bits are exactly same. In addition, according to Lemma 1, the last row of \mathbf{P}_{n-d_o} are all ones. Consequently, when polar encoding $\beta = \hat{\mathbf{u}} \cdot \mathbf{P}_{n-d_o}$ is implemented, u_{N_o-1} will participate in the computation of every element in β . If the value of u_{N_o-1} is reversed, every element in β will also be reversed, which leads to $\beta_0 \oplus \beta_1 = \mathbf{0}$. ■

Since only an information bit is included in the Rev node, only one path split is needed for list decoding. And by Theorem 1, we can get an efficient algorithm as expressed in Algorithm 3. The $N_o - 1$ frozen bits $v_i, i = 0, \dots, N_o - 2$ should be set to 0 firstly. The information bit v_{N_o-1} results in the path expansion of each path, and comparing α with β , we can compute the PMs on the top of the subtree. Notice that Theorem 1 can simplify the computation of β . Eventually, after path elimination, we can get v_{N_o-1} of each path.

D. SPC Nodes

We say that a node o is a SPC node if the first bit v_0 in \mathbf{v} is a frozen bit while the last $N_o - 1$ bits are information bits. Fig. 4 depicts the SPC nodes in yellow parallelograms.

Lemma 2: The first row of $\mathbf{P}_n, n \geq 1$ contains only one 1 at the first position while other rows contain even number of ones. We can formulate this expression as

$$\begin{aligned}
 P_n(0, 0) &= 1, P_n(0, j) = 0, 1 \leq j \leq 2^n - 1 \\
 \bigoplus_{j=0}^{2^n-1} P_n(i, j) &= 0, 1 \leq i \leq 2^n - 1
 \end{aligned} \tag{8}$$

Algorithm 3 Fast List Decoding of a Rev Node o

Input: $\alpha[l], s[l], PM_l, l = 0, \dots, L-1, \mathbf{P}_{n-d_o}, \mathbf{c}$
Output: $\beta[l], s[l], PM_l, \hat{\mathbf{v}}[l], \hat{\mathbf{u}}[l], l = 0, \dots, L-1$

```

1: for  $l \leftarrow 0$  to  $L-1$  do
2:   for  $i \leftarrow 0$  to  $N_o-2$  do
3:      $\hat{v}_i[l] \leftarrow 0$ 
4:      $[\hat{u}_i[l], s[l]] \leftarrow \text{conv1bitEnc}(\hat{v}_i[l], s[l], \mathbf{c})$ 
5:   end for
6: end for
7: for  $l \leftarrow 0$  to  $L-1$  do
8:    $ll = l + L$ 
9:    $[s'[l], s'[ll]] \leftarrow [s[l], s[l]]$ 
10:   $[\hat{\mathbf{v}}'[l], \hat{\mathbf{v}}'[ll]] \leftarrow [\hat{\mathbf{v}}[l], \hat{\mathbf{v}}[ll]]$ 
11:   $[\hat{\mathbf{u}}'[l], \hat{\mathbf{u}}'[ll]] \leftarrow [\hat{\mathbf{u}}[l], \hat{\mathbf{u}}[ll]]$ 
12:   $[\hat{v}'_{N_o-1}[l], \hat{v}'_{N_o-1}[ll]] \leftarrow [0, 1]$ 
13:   $[\hat{u}'_{N_o-1}[l], s'[ll]] \leftarrow \text{conv1bitEnc}(\hat{v}'_{N_o-1}[l], s'[ll], \mathbf{c})$ 
14:   $[\hat{u}'_{N_o-1}[ll], s'[ll]] \leftarrow \text{conv1bitEnc}(\hat{v}'_{N_o-1}[ll], s'[ll], \mathbf{c})$ 
15:   $\beta'[l] \leftarrow \hat{\mathbf{u}}'[l] \cdot \mathbf{P}_{n-d_o}$ 
16:   $\beta'[ll] \leftarrow \mathbf{1} - \beta'[l]$ 
17:   $PM'_l \leftarrow \text{calcPM}(PM_l, \alpha[l], \beta'[l], N_o)$ 
18:   $PM'_{ll} \leftarrow \text{calcPM}(PM_l, \alpha[l], \beta'[ll], N_o)$ 
19: end for
20:  $[\widetilde{\mathbf{PM}}, \widetilde{\mathbf{I}}] \leftarrow \text{sort}([PM'_0, \dots, PM'_{2L-1}], \text{'ascend'})$ 
21: for  $l \leftarrow 0$  to  $L-1$  do
22:    $PM_l \leftarrow \widetilde{PM}_l$ 
23:    $s[l] \leftarrow s'[l]$ 
24:    $\beta[l] \leftarrow \beta'[l]$ 
25:    $\hat{\mathbf{u}}[l] \leftarrow \hat{\mathbf{u}}'[l]$ 
26:    $\hat{\mathbf{v}}[l] \leftarrow \hat{\mathbf{v}}'[l]$ 
27: end for

```

Proof: We prove this lemma by induction. When $n = 1$, we have $\mathbf{P}_1 = \mathbf{P} = [1, 0; 1, 1]$, the lemma holds. Then we suppose this lemma holds for $n-1, n \geq 2$. According to (6), the first half rows in \mathbf{P}_n are constructed by concatenation \mathbf{P}_{n-1} with 0, while the second half rows in \mathbf{P}_n are constructed by concatenation \mathbf{P}_{n-1} twice. Hence, the number of ones of the first half rows in \mathbf{P}_n are the same as \mathbf{P}_{n-1} while the number of ones of the second half rows in \mathbf{P}_n are even. Since we have assumed that the first row of \mathbf{P}_{n-1} contains only one 1 at the first position while other rows contain even number of ones, we can get that the first row of \mathbf{P}_n contains only one 1 at the first position while other rows contain even number of ones. ■

Based on Lemma 2, we can obtain the following theorem for SPC nodes.

Theorem 2: As for a SPC node o , the bit vector β will satisfy

$$\bigoplus_{j=0}^{N_o-1} \beta_j = u_0 \quad (9)$$

Proof: According to matrix multiplication, we have

$$\begin{aligned}
\bigoplus_{j=0}^{N_o-1} \beta_j &= \bigoplus_{j=0}^{N_o-1} \bigoplus_{i=0}^{N_o-1} u_i P(i, j) \\
&= \bigoplus_{i=0}^{N_o-1} u_i \bigoplus_{j=0}^{N_o-1} P(i, j) \\
&= (u_0 \bigoplus_{j=0}^{N_o-1} P(0, j)) \oplus (\bigoplus_{i=1}^{N_o-1} u_i \bigoplus_{j=0}^{N_o-1} P(i, j)) \\
&= u_0
\end{aligned} \quad (10)$$

The last equation is obtained by substituting (8). ■

When the list decoder reaches a SPC node o , the frozen bit v_0 should be set to 0 and u_0 can be immediately obtained by 1-bit convolutional encoding. After the hard decision of α , we can use β and u_0 to get the check value

$$\gamma = \bigoplus_{j=0}^{N_o-1} \beta_j \oplus u_0 \quad (11)$$

To keep $\gamma = 0$, the least reliable bit should first decide whether to reverse and then two bits need to be reversed at the same time. The exact number of path splits to preserve the same performance as list decoding is $\binom{N_o}{2} = N_o(N_o-1)/2$, which is quadratic with N_o and it is more complex than the time required by list decoding which is linear with N_o [6]. However, an approximate algorithm will limit the number of path splits to $\min(L-1, N_o-1)$, which is so effective that the performance loss is negligible [8]. The details of the fast list decoding of a SPC node o are exhibited in Algorithm 4. First, the absolute values in α are sorted and then the least reliable bit which corresponds to the parity check constraint is decoded. Then $t = \min(L-1, N_o-1)$ path splits are implemented to judge $\tilde{\alpha}_i, i = 1, \dots, t$. Whereafter, other bits in β can be directly judged by their corresponding LLRs in α . Note that after all other bits are obtained, the least reliable bit needs to be recalculated based on (11). Ultimately, \mathbf{u} can be calculated through the inverse process of polar encoding and subsequently \mathbf{v} can be calculated through the inverse process of convolutional encoding.

E. Time Steps

Comparing list decoding with fast list decoding, we give the analysis of the required time steps for the four types of constituent nodes. We hypothesize that the f operation (2), the g operation (3) and one path split all consume one time step. Moreover, we ignore the time step of polar encoding and convolutional encoding. In addition, we do not take into account the resource constraint, which means that all parallel operations can be carried out in one time step. In fact, these are reasonable hypotheses commonly used by scholars [2], [4].

- **Rate-0 Nodes:** The original number of time steps is $2N_o-2$ consisting of N_o-1 f operations and N_o-1 g operations, while the fast list decoding can reduce it to 1 because no f and g operation is needed and there is only one PM computation for a vector.

Algorithm 4 Fast List Decoding of a SPC Node o

Input: $\alpha[l], s[l], PM_l, l = 0, \dots, L-1, \mathbf{P}_{n-d_o}, \mathbf{c}$
Output: $\beta[l], s[l], PM_l, \hat{v}_0[l], \hat{u}_0[l], l = 0, \dots, L-1$

```

1: for  $l \leftarrow 0$  to  $L-1$  do
2:    $\hat{v}_0[l] \leftarrow 0$ 
3:    $[\hat{u}_0[l], s[l]] \leftarrow \text{conv1bitEnc}(\hat{v}_0[l], s[l], \mathbf{c})$ 
4:    $\beta[l] \leftarrow \frac{1}{2}(1 - \text{sgn}(\alpha[l]))$ 
5:    $\gamma[l] \leftarrow (\sum_{j=0}^{N_o-1} \beta_j[l] + \hat{u}_0[l]) \% 2$ 
6:    $[\tilde{\alpha}[l], \tilde{\mathbf{I}}[l]] \leftarrow \text{sort}(|\alpha[l]|, \text{'ascend'})$ 
7:   if  $\gamma[l] = 0$  then
8:      $PM_l = PM_l$ 
9:   else
10:     $PM_l = PM_l + |\tilde{\alpha}_0[l]|$ 
11:   end if
12: end for
13: for  $i \leftarrow 1$  to  $\min(L-1, N_o-1)$  do
14:   for  $l \leftarrow 0$  to  $L-1$  do
15:      $ll = l + L$ 
16:      $[\hat{u}'_0[l], \hat{u}'_0[ll]] \leftarrow [\hat{u}_0[l], \hat{u}_0[ll]]$ 
17:      $[\gamma'[l], \gamma'[ll]] \leftarrow [\gamma[l], \gamma[ll]]$ 
18:      $[\beta'[l], \beta'[ll]] \leftarrow [\beta[l], \beta[ll]]$ 
19:      $[s'[l], s'[ll]] \leftarrow [s[l], s[ll]]$ 
20:      $[\tilde{\alpha}'[l], \tilde{\alpha}'[ll]] \leftarrow [\tilde{\alpha}[l], \tilde{\alpha}[ll]]$ 
21:      $[\tilde{\mathbf{I}}'[l], \tilde{\mathbf{I}}'[ll]] \leftarrow [\tilde{\mathbf{I}}[l], \tilde{\mathbf{I}}[ll]]$ 
22:      $[\beta'_i[l], \beta'_i[ll]] \leftarrow [0, 1]$ 
23:      $PM'_l \leftarrow \text{calcPM2}(PM_l, \tilde{\alpha}'_i[l], \beta'_i[l], 1, \gamma'_i[l], \tilde{\alpha}_0)$ 
24:      $PM'_{ll} \leftarrow \text{calcPM2}(PM_l, \tilde{\alpha}'_i[ll], \beta'_i[ll], 1, \gamma'_i[ll], \tilde{\alpha}_0)$ 
25:   end for
26:    $[\tilde{\mathbf{P}}\mathbf{M}, \tilde{\mathbf{I}}] \leftarrow \text{sort}([PM'_0, \dots, PM'_{2L-1}], \text{'ascend'})$ 
27:   for  $l \leftarrow 0$  to  $L-1$  do
28:      $PM_l \leftarrow \tilde{\mathbf{P}}\mathbf{M}_l$ 
29:      $\tilde{\mathbf{I}}[l] \leftarrow \tilde{\mathbf{I}}'[l]$ 
30:      $\tilde{\alpha}[l] \leftarrow \tilde{\alpha}'[l]$ 
31:      $s[l] \leftarrow s'[l]$ 
32:      $\beta[l] \leftarrow \beta'[l]$ 
33:      $\beta_{\tilde{\mathbf{I}}}[l] \leftarrow \beta'_{\tilde{\mathbf{I}}}[l]$ 
34:      $\gamma[l] \leftarrow \gamma'[l]$ 
35:      $\hat{u}_0[l] \leftarrow \hat{u}'_0[l]$ 
36:   end for
37: end for
38: for  $l \leftarrow 0$  to  $L-1$  do
39:    $\beta_{\tilde{\mathbf{I}}_0}[l] \leftarrow (\sum_{j=1}^{N_o-1} \beta_{\tilde{\mathbf{I}}_j}[l] + \hat{u}_0[l]) \% 2$ 
40:    $\hat{\mathbf{u}}[l] \leftarrow \beta[l] \cdot \mathbf{P}_{n-d_o}$ 
41:   for  $i \leftarrow 0$  to  $N_o-1$  do
42:      $[\hat{v}_i[l], s[l]] \leftarrow \text{conv1bitInvEnc}(\hat{u}_i[l], s[l], \mathbf{c})$ 
43:   end for
44: end for

```

- **Rate-1 Nodes:** The original number of time steps is $3N_o - 2$ consisting of $N_o - 1$ f operations, $N_o - 1$ g operations and N_o path splits, while the fast list decoding can reduce it to $\min\{L-1, N_o\}$ with an effective algorithm for path split.
- **Rev Nodes:** The original number of time steps is $2N_o - 1$ consisting of $N_o - 1$ f operations, $N_o - 1$ g operations and one path split, while the fast list decoding can reduce

TABLE I
TIME STEPS OF THE FOUR CONSTITUENT NODES FOR LIST DECODING AND FAST LIST DECODING

Constituent Node	List Decoding	Fast List Decoding
Rate-0	$2N_o - 2$	1
Rate-1	$3N_o - 2$	$\min\{L-1, N_o\}$
Rev	$2N_o - 1$	2
SPC	$3N_o - 3$	$\min\{L, N_o\} + 1$

it to 2 with one path split and one PM computation for a vector.

- **SPC Nodes:** The original number of time steps is $3N_o - 3$ consisting of $N_o - 1$ f operations, $N_o - 1$ g operations and $N_o - 1$ path splits, while the fast list decoding can reduce it to $\min\{L, N_o\} + 1$ with one bit estimate for the least reliable bit, $\min\{L-1, N_o-1\}$ path splits and one bit recalculation.

Time steps of the four constituent nodes for list decoding and fast list decoding is listed in Table I. One thing that needs to be emphasized is that the performance of fast list decoding of Rate-0, Rate-1 and Rev nodes is exactly equivalent to that of list decoding, while the fast list decoding algorithm for SPC nodes is an approximation algorithm. Nevertheless, the performance loss is so small as to be negligible as shown in Section IV.

IV. SIMULATION RESULTS

In this section, we provide the simulation results of the fast list decoding under different code lengths, code rates and list sizes. All PAC codes are obtained via RM rate-profiling using the rate-1 convolutional code generated by $\mathbf{c} = (1, 0, 1, 1, 0, 1, 1)$, just as the parameter setting in [9]. The encoded codeword \mathbf{x} is modulated by binary phase shift keying (BPSK) modulation and transmitted over binary-input additive white Gaussian noise (BI-AWGN) channel. The BI-AWGN dispersion bound are obtained from [12]. We measure the FER performance against the E_b/N_0 in dB, where E_b denotes the bit energy and N_0 denotes the power spectral density of the BI-AWGN noise. For each E_b/N_0 , we ensure that at least 500 error frames occur to keep the results reliable. For the sake of concision, we refer to list decoding, fast list decoding with three types of constituent nodes (Rate-0 nodes, Rate-1 Nodes and Rev nodes) and four types of constituent nodes (Rate-0 nodes, Rate-1 Nodes, Rev nodes and SPC nodes) as ‘List’, ‘Fast-List-Three’ and ‘Fast-List-Four’, respectively.

At the beginning, we investigate the FER performance comparison of List, Fast-List-Three and Fast-List-Four for PAC(128, 64) under different list sizes, as shown in Fig. 5. The BI-AWGN dispersion bound (128, 64) is also displayed. According to the analysis in Section III, Fast-List-Three is absolutely equivalent to List and Fast-List-Four is an approximation in theory. From Fig. 5, we can see that the simulation results exactly correspond to the theory. Fast-List-Three yields the same performance with List regardless of L and approaches the BI-AWGN dispersion bound when $L = 256$ with only 0.1 dB gap at FER 10^{-3} . To our excitement, Fast-List-Four incurs no performance degradation

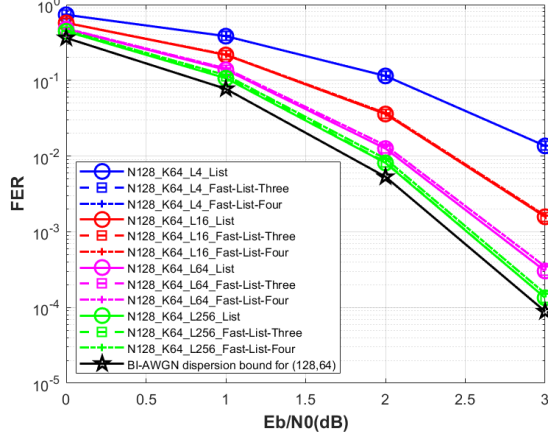


Fig. 5. The FER performance comparison of List, Fast-List-Three and Fast-List-Four for $PAC(128, 64)$ under different list sizes. The BI-AWGN dispersion bound for $(128, 64)$ is also displayed.

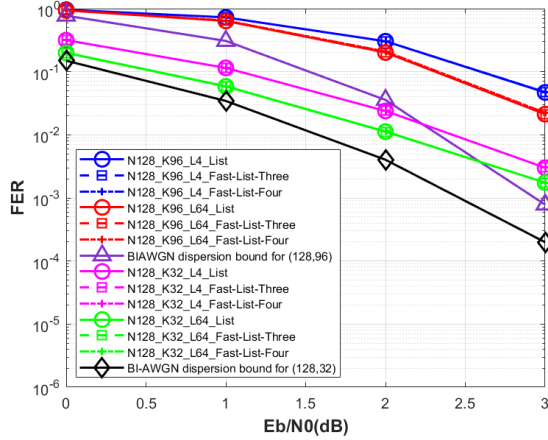


Fig. 6. The FER performance comparison of List, Fast-List-Three and Fast-List-Four for $PAC(128, 32)$ and $PAC(128, 96)$ under different list sizes. The two BI-AWGN dispersion bounds are also displayed.

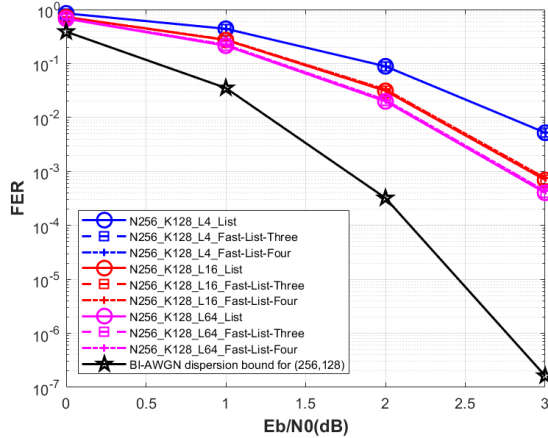


Fig. 7. The FER performance comparison of List, Fast-List-Three and Fast-List-Four for $PAC(256, 128)$ under different list sizes. The BI-AWGN dispersion bound for $(256, 128)$ is also displayed.

TABLE II
TIME STEPS OF LIST DECODING AND FAST LIST DECODING UNDER DIFFERENT CODE LENGTHS, CODE RATES AND LIST SIZES.

Code Parameter	L	List Decoding	Fast-List-Three Decoding (Reduction)	Fast-List-Four Decoding (Reduction)
$PAC(128, 32)$ $R = 1/4$	4	286	75 (73.78%)	72 (74.83%)
	64	286	81 (71.68%)	78 (72.73%)
$PAC(128, 64)$ $R = 1/2$	4	318	143 (55.03%)	108 (66.04%)
	16	318	152 (52.2%)	132 (58.49%)
	64	318	152 (52.2%)	132 (58.49%)
$PAC(128, 96)$ $R = 3/4$	4	350	145 (58.57%)	86 (75.43%)
	64	350	179 (48.85%)	150 (57.14%)
$PAC(256, 128)$ $R = 1/2$	4	638	233 (63.48%)	163 (74.45%)
	16	638	267 (58.15%)	215 (66.3%)
	64	638	268 (57.99%)	231 (63.79%)

when $L = 4$ and $L = 16$, and causes neglectable performance loss when $L = 64$ and $L = 256$.

Afterwards, we fix the code length and change the code rate. Fig. 6 presents the FER performance comparison of List, Fast-List-Three and Fast-List-Four for $PAC(128, 32)$ and $PAC(128, 96)$ under different list sizes. The two BI-AWGN dispersion bounds are also displayed. We make sure that the performance of $PAC(128, 32)$ and $PAC(128, 96)$ has converged when $L = 64$. It can be observed that all curves of Fast-List-Three and Fast-List-Four coincide with that of List. However, the convergent performance is inferior to the BI-AWGN bound with 0.5 dB gap at FER 10^{-2} for $PAC(128, 32)$ and 0.8 dB gap at FER 10^{-1} for $PAC(128, 96)$.

In the end, we fix the code rate and adjust the code length. The FER performance comparison of List, Fast-List-Three and Fast-List-Four for $PAC(256, 128)$ under different list sizes is depicted in Fig. 7. The BI-AWGN dispersion bound for $(256, 128)$ is also displayed. Both Fast-List-Three and Fast-List-Four achieve the same performance as the list decoding. However, the convergent performance of PAC codes with $L = 64$ is so far from the dispersion bound. More advanced techniques to improve PAC codes with long code lengths are urgently needed.

To illustrate the speed advantage of the proposed fast list decoders, we summarize the time steps of list decoding and fast list decoding under different code lengths, code rates and list sizes in Table II. From the table, we can observe that:

- When N and R are fixed, a smaller L will lead to a larger reduction for both Fast-List-Three and Fast-List-Four. The reason is that the fast list decoding of Rate-1 and SPC nodes has taken into account the effect of L , and smaller L will lead to fewer time steps. When L increases, the number of times steps will converge to a constant.
- When N and L are fixed, a lower R tends to result in larger reduction for both Fast-List-Three and Fast-List-Four. The reason is that when the rate is lower, the number of Rate-0 and Rev nodes will become larger. The required times steps of Rate-0 and Rev nodes for fast list

decoding are 1 and 2 respectively, which are so small that bigger gain will be brought about.

- When N and L are fixed, Fast-List-Four has a greater advantage over Fast-List-Three if R is higher. This is obvious because a higher R will lead to more SPC nodes, and hence the fast list decoding algorithm of SPC nodes will show its superiority.
- When R and L are fixed, a bigger N will lead to a larger reduction for both Fast-List-Three and Fast-List-Four. It is easy to think that when the N increases, more constituent nodes will appear and therefore we can further accelerate decoding using our fast algorithms.

V. CONCLUSION

In this paper, we propose fast list decoders for PAC codes. The fast scheme is mainly based on tree pruning technique which decodes constituent nodes on the top of the subtree without traversal of the binary tree. Fast list decoding algorithms of Rate-0, Rate-1 and Rev nodes are exactly equivalent to that of list decoding, while that of SPC nodes is an approximation. Consequently, the FER results demonstrate that fast list decoding with three types of constituent nodes incurs no performance degradation while the introduction of SPC nodes causes negligible performance loss. As the most remarkable superiority, the proposed decoders can significantly reduce the number of time steps so as to speed decoding in practice.

As for the future direction, more constituent nodes may be found to further reduce the decoding latency. Besides, we have observed that the performance of PAC codes is still far from the dispersion bound when the code length increases to 256. More improvements about encoding and decoding are in demand to enhance the application universality of PAC codes.

APPENDIX A SUBROUTINES

Algorithm 5 provides these subroutines required for algorithms in Section III.

REFERENCES

- [1] E. Arıkan, "Channel polarization: A method for constructing capacity-achieving codes for symmetric binary-input memoryless channels," *IEEE Transactions on Information Theory*, vol. 55, no. 7, pp. 3051–3073, July 2009.
- [2] C. Leroux, A. J. Raymond, G. Sarkis, and W. J. Gross, "A semi-parallel successive-cancellation decoder for polar codes," *IEEE Transactions on Signal Processing*, vol. 61, no. 2, pp. 289–299, 2013.
- [3] I. Tal and A. Vardy, "List decoding of polar codes," *IEEE Transactions on Information Theory*, vol. 61, no. 5, pp. 2213–2226, May 2015.
- [4] A. Balatsoukas-Stimming, M. B. Parizi, and A. Burg, "Llr-based successive cancellation list decoding of polar codes," *IEEE Transactions on Signal Processing*, vol. 63, no. 19, pp. 5165–5179, 2015.
- [5] S. A. Hashemi, C. Condo, and W. J. Gross, "Simplified successive-cancellation list decoding of polar codes," in *2016 IEEE International Symposium on Information Theory (ISIT)*, 2016, pp. 815–819.
- [6] —, "A fast polar code list decoder architecture based on sphere decoding," *IEEE Transactions on Circuits and Systems I: Regular Papers*, vol. 63, no. 12, pp. 2368–2380, 2016.
- [7] —, "Fast simplified successive-cancellation list decoding of polar codes," in *2017 IEEE Wireless Communications and Networking Conference Workshops (WCNCW)*, 2017, pp. 1–6.

Algorithm 5 Subroutines

```

1: subroutine conv1bitEnc( $v, s, c$ )
2:  $u \leftarrow v \cdot c_0$ 
3: for  $i \leftarrow 1$  to  $m$  do
4:   if  $c_i = 1$  then
5:      $u \leftarrow u \oplus s_{i-1}$ 
6:   end if
7: end for
8:  $s \leftarrow [v, s_0, \dots, s_{m-2}]$ 
9: return  $u, s$ 
10:
11: subroutine conv1bitInvEnc( $u, s, c$ )
12:  $v \leftarrow 0$ 
13:  $u\_temp \leftarrow v \cdot c_0$ 
14: for  $i \leftarrow 1$  to  $m$  do
15:   if  $c_i = 1$  then
16:      $u\_temp \leftarrow u\_temp \oplus s_{i-1}$ 
17:   end if
18: end for
19: if  $u\_temp = u$  then
20:    $v \leftarrow 0$ 
21: else
22:    $v \leftarrow 1$ 
23: end if
24:  $s \leftarrow [v, s_0, \dots, s_{m-2}]$ 
25: return  $v, s$ 
26:
27: subroutine calcPM( $PM, \alpha, \beta, len$ )
28: for  $i \leftarrow 0$  to  $len - 1$  do
29:   if  $\beta_i = \frac{1}{2}(1 - \text{sgn}(\alpha_i))$  then
30:      $PM = PM$ 
31:   else
32:      $PM = PM + |\alpha_i|$ 
33:   end if
34: end for
35: return  $PM$ 
36:
37: subroutine calcPM2( $PM, \alpha, \beta, len, \gamma, \tilde{\alpha}_0$ )
38: for  $i \leftarrow 0$  to  $len - 1$  do
39:   if  $\beta_i = \frac{1}{2}(1 - \text{sgn}(\alpha_i))$  then
40:      $PM = PM$ 
41:   else
42:      $PM = PM + |\alpha_i| + (1 - 2\gamma)|\tilde{\alpha}_0|$ 
43:   end if
44: end for
45: return  $PM$ 

```

- [8] —, "Fast and flexible successive-cancellation list decoders for polar codes," *IEEE Transactions on Signal Processing*, vol. 65, no. 21, pp. 5756–5769, 2017.
- [9] E. Arıkan, "From sequential decoding to channel polarization and back again," *arXiv e-prints*, p. arXiv:1908.09594, Aug. 2019.
- [10] P. Elias, "Coding for noisy channels," *IRE Conv. Rec.*, pp. 37–47, 1955.
- [11] R. Fano, "A heuristic discussion of probabilistic decoding," *IEEE Transactions on Information Theory*, vol. 9, no. 2, pp. 64–74, 1963.
- [12] Y. Polyanskiy, H. V. Poor, and S. Verdú, "Channel coding rate in the finite blocklength regime," *IEEE Transactions on Information Theory*, vol. 56, no. 5, pp. 2307–2359, 2010.
- [13] M. Rowshan, A. Burg, and E. Viterbo, "Polarization-adjusted Convolutional (PAC) Codes: Fano Decoding vs List Decoding," *arXiv e-prints*,

- p. arXiv:2002.06805, Feb. 2020.
- [14] H. Yao, A. Fazeli, and A. Vardy, "List Decoding of Arikan's PAC Codes," *arXiv e-prints*, p. arXiv:2005.13711, May 2020.
 - [15] I. Reed, "A class of multiple-error-correcting codes and the decoding scheme," *Transactions of the IRE Professional Group on Information Theory*, vol. 4, no. 4, pp. 38–49, 1954.
 - [16] D. E. Muller, "Application of boolean algebra to switching circuit design and to error detection," *Transactions of the I.R.E. Professional Group on Electronic Computers*, vol. EC-3, no. 3, pp. 6–12, 1954.
 - [17] P. Trifonov and V. Miloslavskaya, "Polar codes with dynamic frozen symbols and their decoding by directed search," in *2013 IEEE Information Theory Workshop (ITW)*, 2013, pp. 1–5.
 - [18] L. Li and W. Zhang, "On the encoding complexity of systematic polar codes," in *2015 28th IEEE International System-on-Chip Conference (SOCC)*, 2015, pp. 415–420.